

Out-of-equilibrium self-assembly for the formation of biological and soft-matter structures

Miguel Rubi





Congratulations Signe!!

SKe^{4,25}



Age is just a number!

$\ln 70 = 4.24849524204936$

$\ln 55 = 4.00733318523247$

Three type of ages:

- Official (ID)
- Biological (how do you feel)
- Relativistic (time passes slowly when activity is very intense)

Andres Arango
(UB)



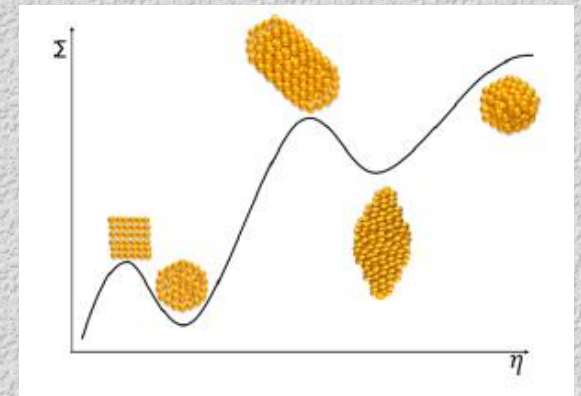
Daniel Barragan
(Univ. Nacional Colombia)



Outline

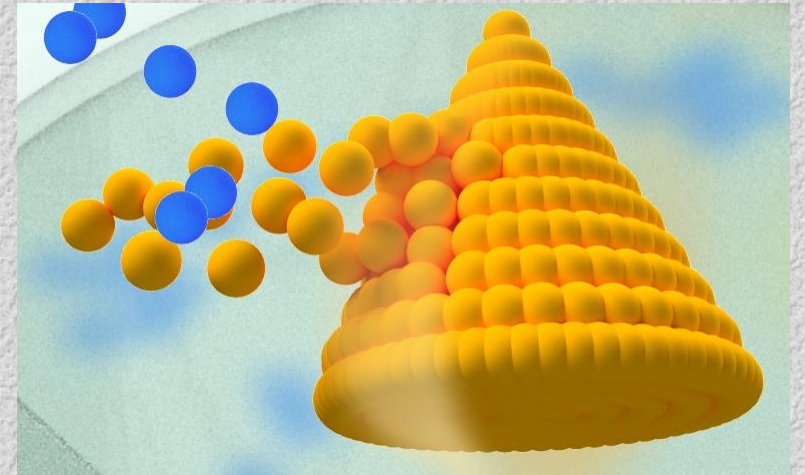
1. Out of equilibrium self-assembly
2. Gelation
3. Liesegang patterns
4. Determining the architecture of self-assembled structures from energy dissipation

$$\eta_{\text{sph}} = \frac{l_a l_b l_c}{\max(l_a, l_b, l_c)^3}$$

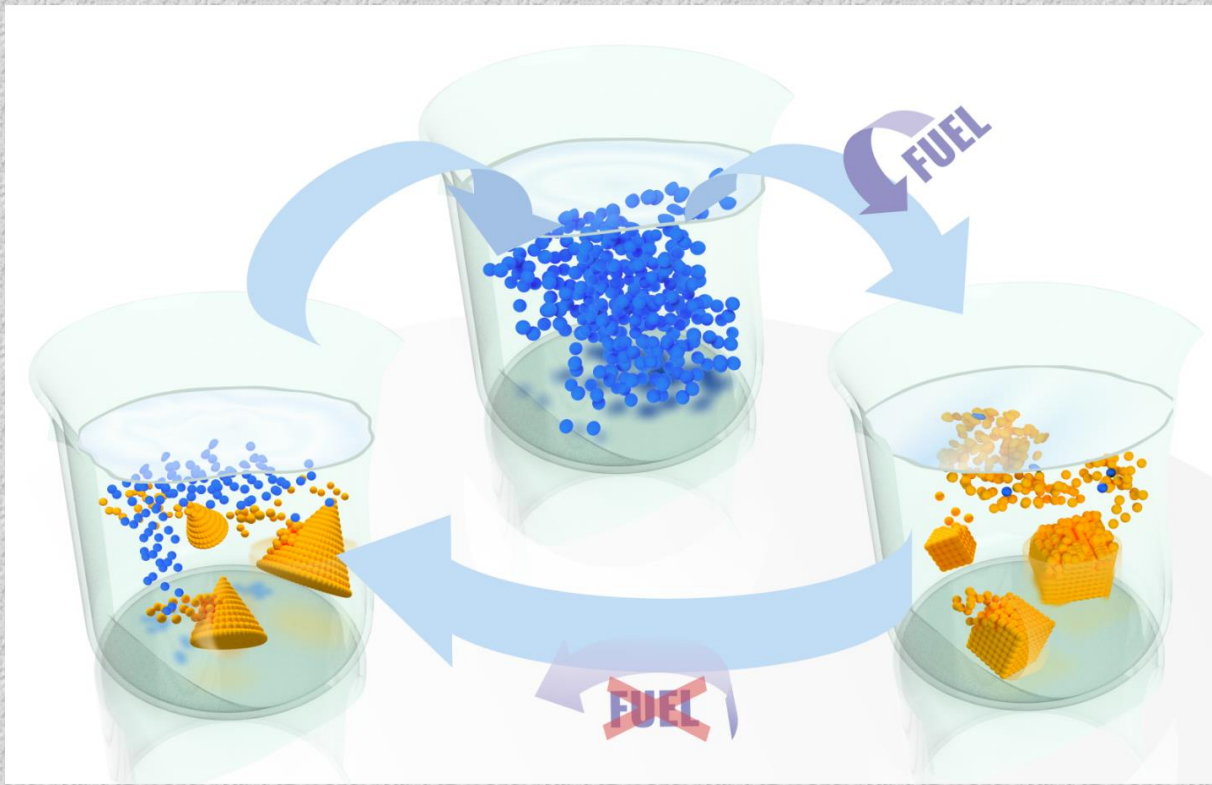


Out-of-equilibrium self-assembly

- ❖ Self-assembly (SA) is the organization of **discrete elements** into **structures**.
- ❖ An assembled structure is an arrangement of **building blocks** (BB) into a **material object** that integrates a heterogeneous system.
- ❖ **Equilibrium SA** leads to the formation of stable structures through **quasi-equilibrium steps**.

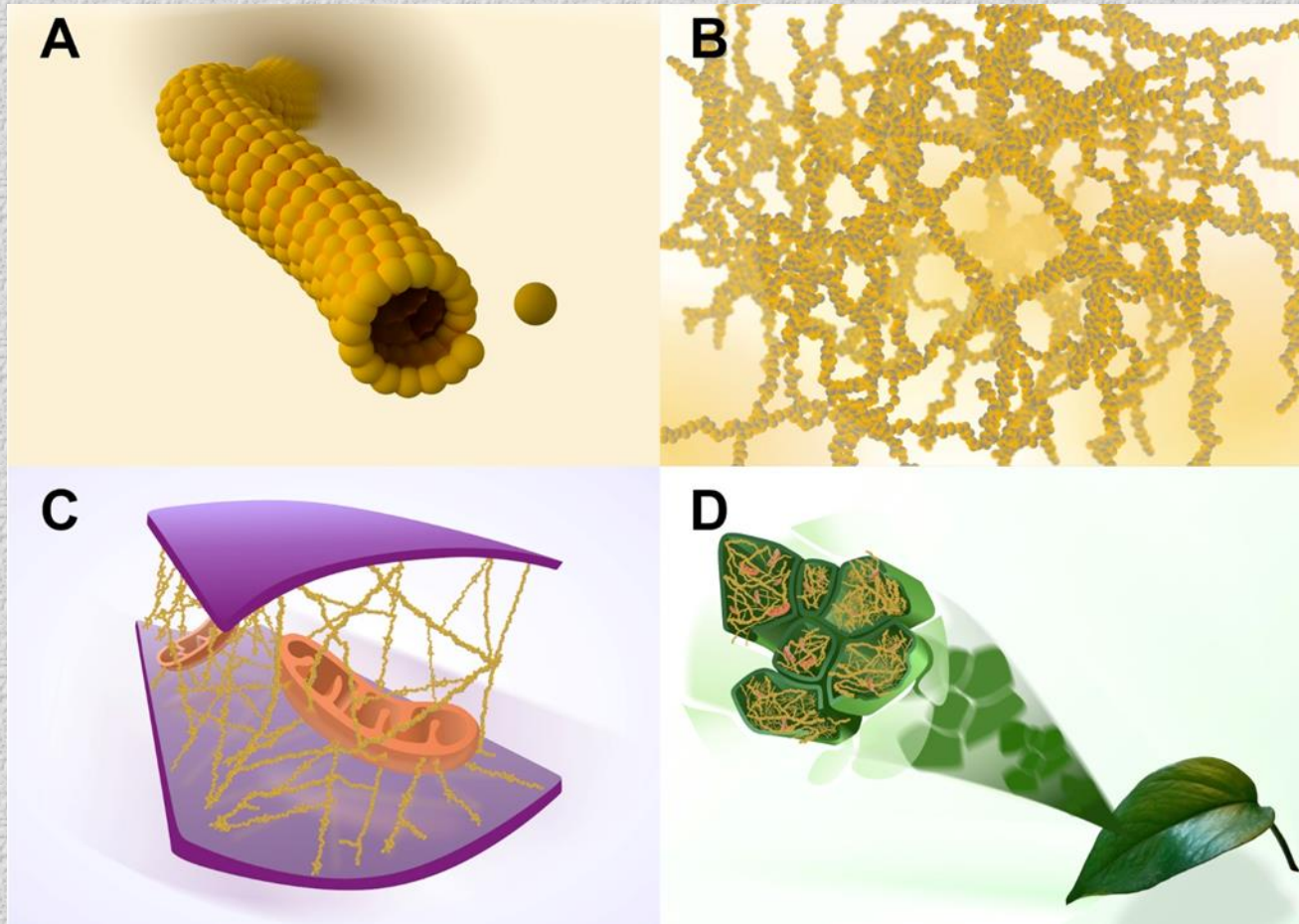


*A. Arango, JMR, D. Barragan, : Phys. Chem. Chem. Phys.,
2019, 21, 17475; Perspective*



- ❖ Nonequilibrium self-assembly (**NESA**) **leads to** the formation of stable, metastable, kinetically-trapped and stationary **structures mediated by dissipation**.
- ❖ **NESA** processes are the **previous steps** in the formation of self-organized (**SO**) structures.

Structures



A: Microtubules, assembled from tubuline dimers.

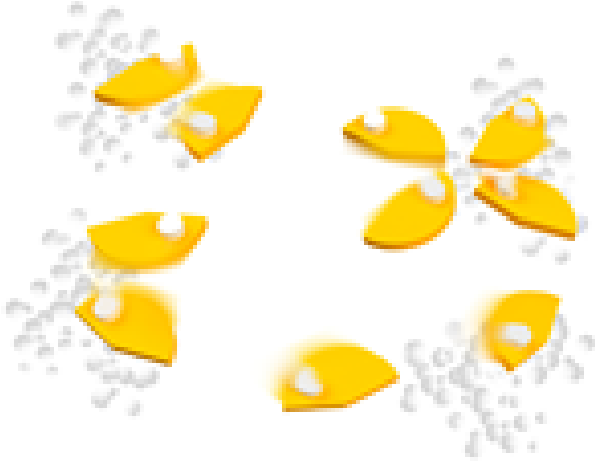
B: Gel, assembled from fibers or microtubules.

C: Plant cells, assembled from microtubules assemblies.

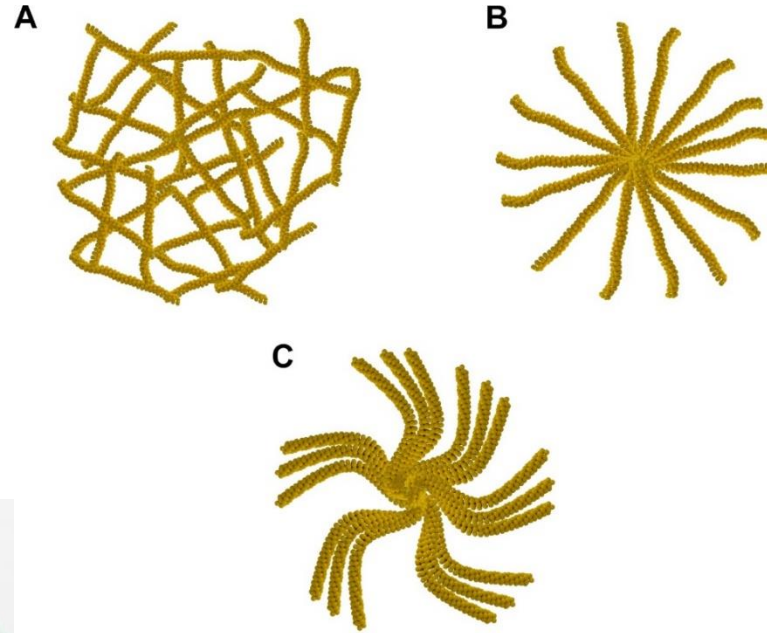
D: Leaf, assembled from plant cells

Structures

Self-propelled “particles”



**Magneto-hydrodynamic
assemblies**

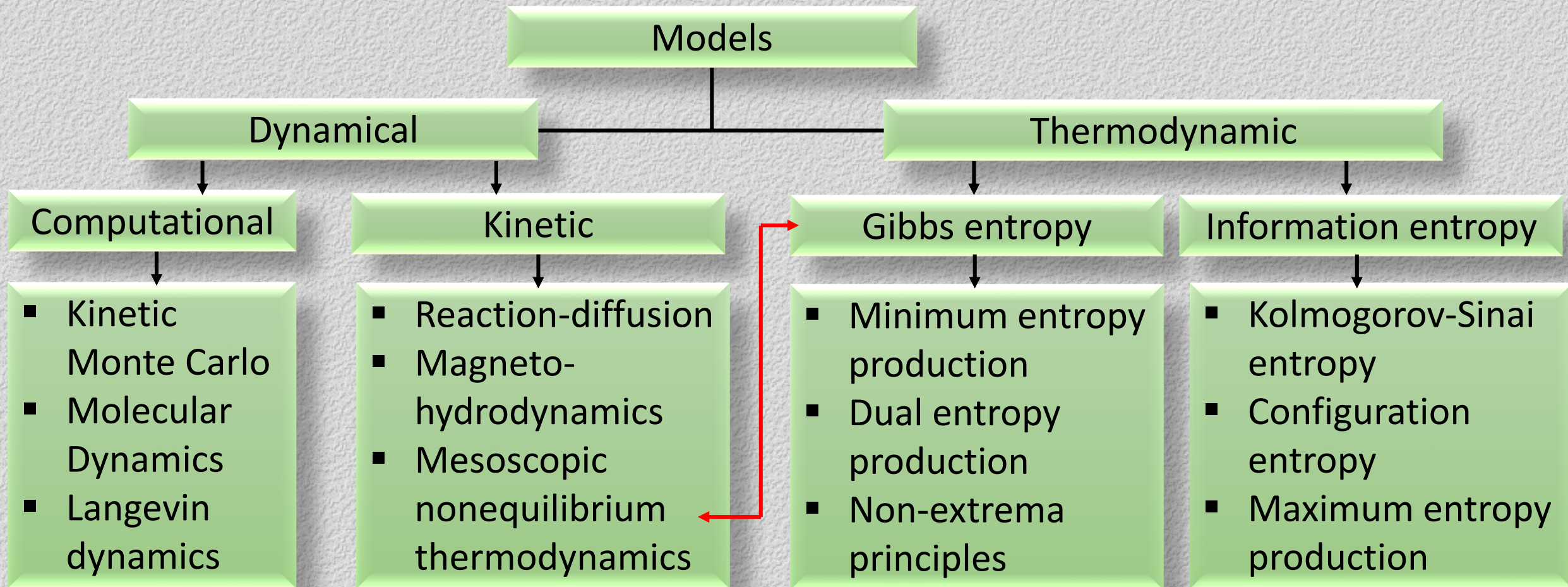


**Microtubule-based
structures, active gels**

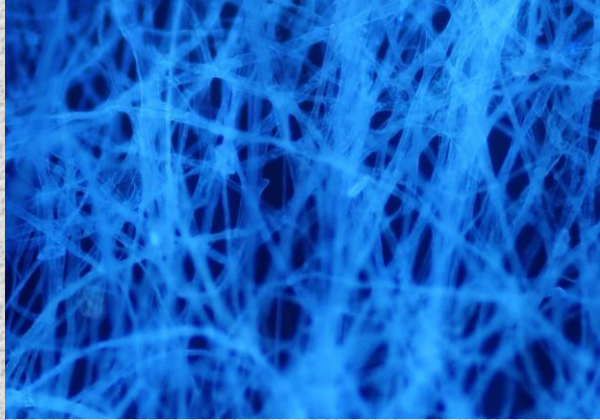
- A. Networks (contractile or as cellular structure)
- B. Microtubule asters
- C. Microtubule vortex

Questions

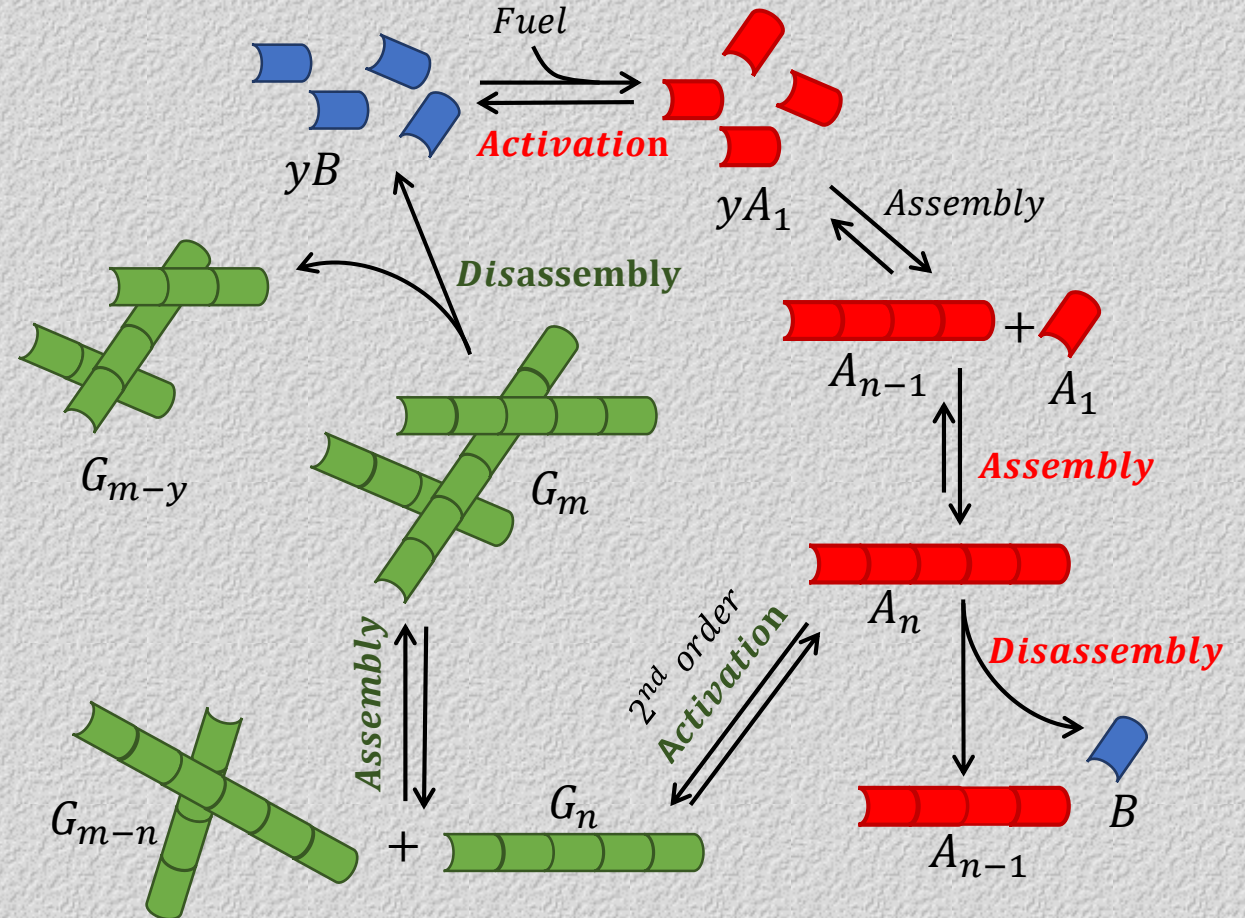
- How the **formation of the structures** is governed by the **laws of thermodynamics**?
- What is the **amount of energy dissipated** in the formation of a non-equilibrium self-assembled structure from a set of disordered elements?
- In the **lack of a non-equilibrium potential** that can constitute a structure selection mechanism, as occurs in equilibrium, we wonder why under specified conditions a determined structure appears and not another.
- **Computational approaches** have technical challenges because the number of particles needed to explain the mesoscale behavior is very large.
- These methods enable the possibility of simulating larger systems for longer time, but they do not enable the **quantification of the dissipation (entropy production)** naturally.



GELATION



- ❖ Gel formation is a NESA process.
- ❖ Model based on mesoscopic nonequilibrium thermodynamics*.
- ❖ The models gives:
 - i) fiber orientation probability
 - ii) dissipation (entropy production).



*D. Reguera, J.M. Rubi, J.M. Vilar, *J. Phys. Chem. B* (2005);
Feature Article

Mechanism

BB: N,N-dibenzoyl-(L)-cystine (DBC)

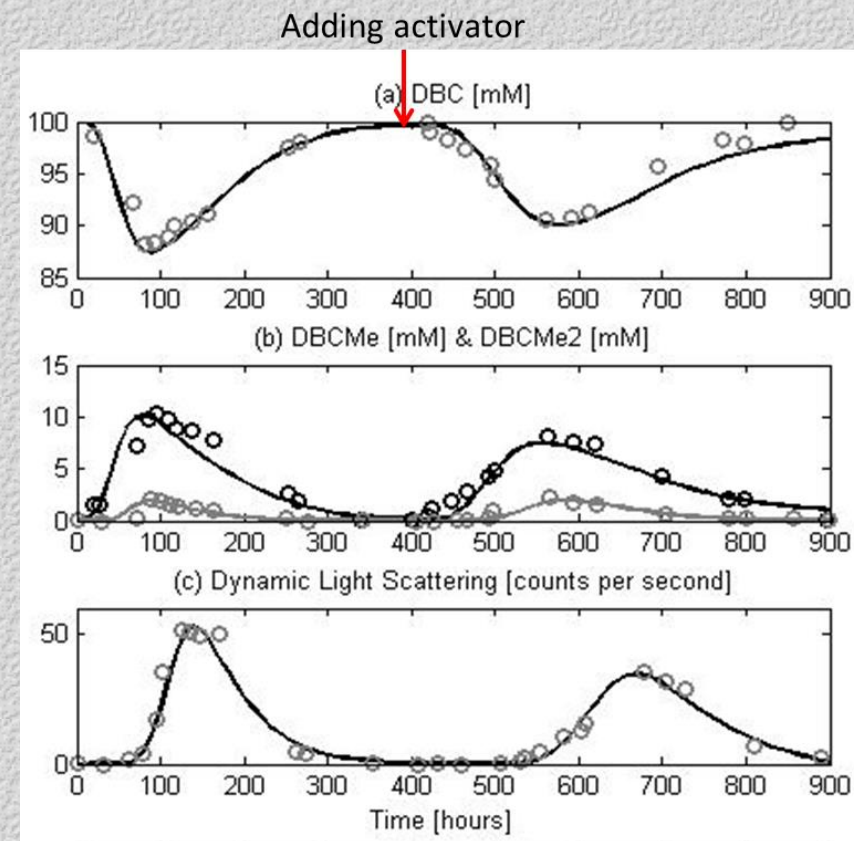
Activator: Methyl Iodide (MeI)

Activated blocks: DBC-Me₂

Intermediate activated BB: DBC-Me

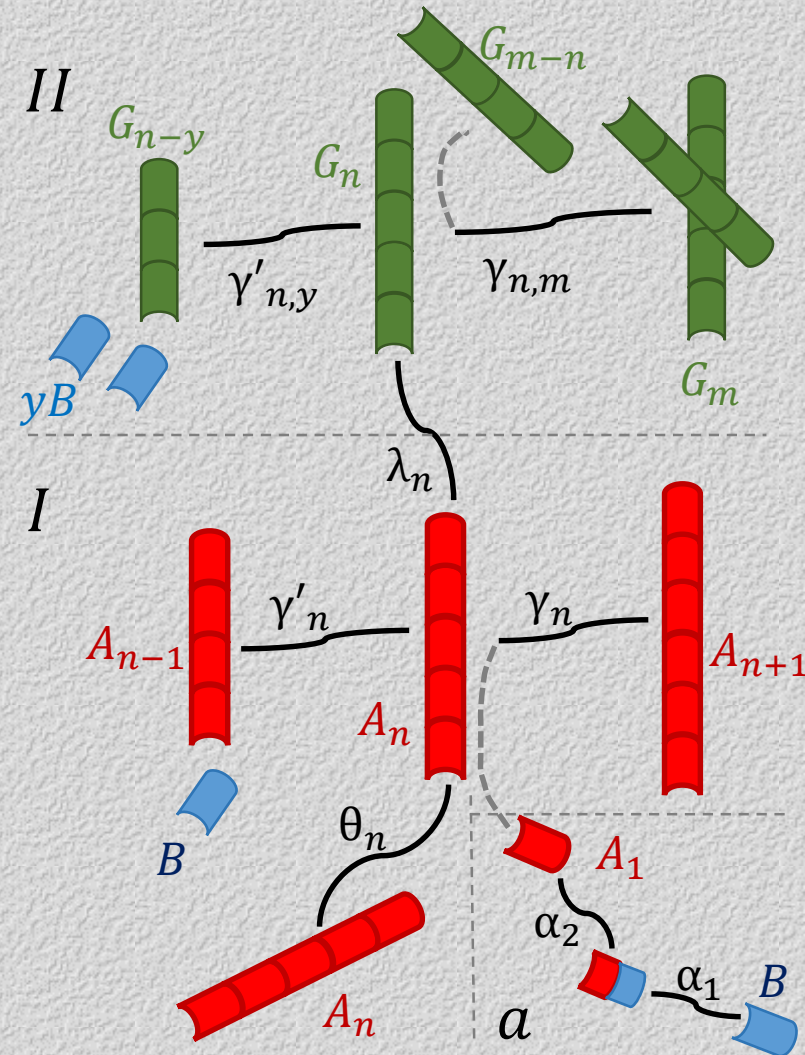
First-order structures: linear fibers formed from DBC by sequential reactions

Second-order structures: gel formed by agglomeration of linear fibers.



A. Arango, JMR, D. Barragan, J. Phys. Chem.B, 122, 4937 (2018)

REACTION COORDINATES



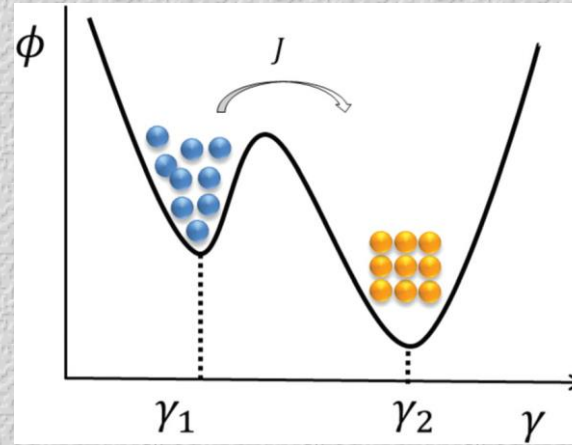


$$\mu_A, \mu_B \rightarrow \mu(\gamma)$$

$$c_A, c_B \rightarrow c(\gamma)$$

$$s \rightarrow s(\gamma)$$

Mesoscopic description:



Reaction
coordinate

$$Tds(\gamma) = -\mu(\gamma)dP(\gamma)$$

Mesoscopic entropy production

J.M. Vilar, J.M. Rubi, PNAS (2001)

$$\sigma(\gamma) = -\frac{1}{T} J(\gamma) \frac{\partial \mu}{\partial \gamma}$$

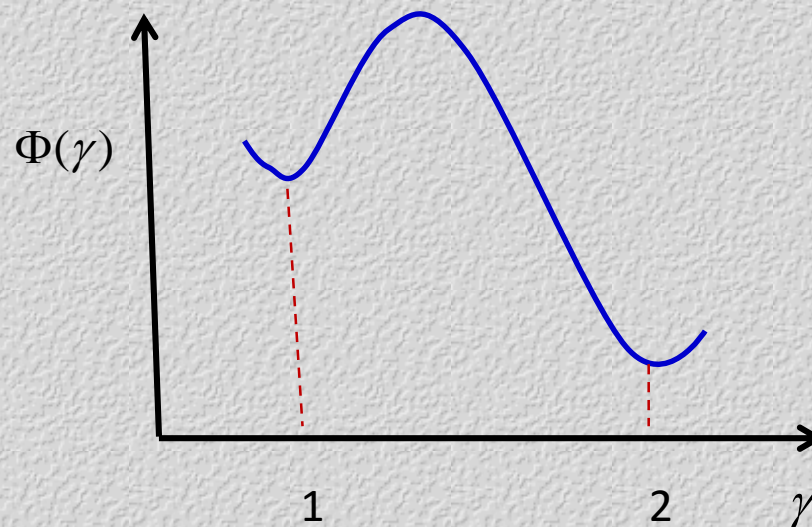
$$J(\gamma) = -\frac{L}{T} \frac{\partial \mu}{\partial \gamma}$$

$$\frac{\partial P}{\partial t} = \frac{\partial}{\partial \gamma} D \left(\frac{\partial P}{\partial \gamma} + \frac{P}{k_B T} \frac{\partial \Phi}{\partial \gamma} \right)$$

$$\mu = k_B T \ln P + \Phi$$

Local fugacity

$$z(\gamma) = e^{\frac{\mu(\gamma)}{k_B T}}$$



$$J = -k_B \frac{L}{z} \frac{\partial z}{\partial \gamma}$$

$$J = -D \frac{\partial z}{\partial \gamma}$$

$$D = k_B \frac{L}{z}$$

$$\bar{J}(t) = \int_1^2 J d\gamma = -D(z_2 - z_1) = -D(e^{\frac{\mu_2}{kT}} - e^{\frac{\mu_1}{kT}})$$

MODEL

Phase Space: $\Gamma_n = (\gamma_n, \gamma'_n, \lambda_n, \theta_n)$

Continuity: $\frac{\partial p_n(\Gamma_n, t)}{\partial t} = -\nabla_{\Gamma_n} \cdot \mathbf{J}_n(\Gamma_n, t)$

**Entropy
production:
(1st order)**

$$\sigma_n = -\frac{1}{T} \sum_{i=1}^4 \int_{\Gamma_n^{(i)}} J_n^{(i)} \frac{\partial \mu_n^{(i)}}{\partial \Gamma_n^{(i)}} d\Gamma_n^{(i)}$$

Current: $J_n^{(i)} = -\frac{L_n^{(ii)}}{T} \frac{\partial \mu_n^{(i)}}{\partial \Gamma_n^{(i)}}$

Chemical potential:

$$\mu_n^{(i)}(\Gamma_n^{(i)}, t) = RT \ln(\psi_n^{(i)} p_n^{(i)}) + \phi_n^{(i)}(\Gamma_n^{(i)})$$

First-order structures:

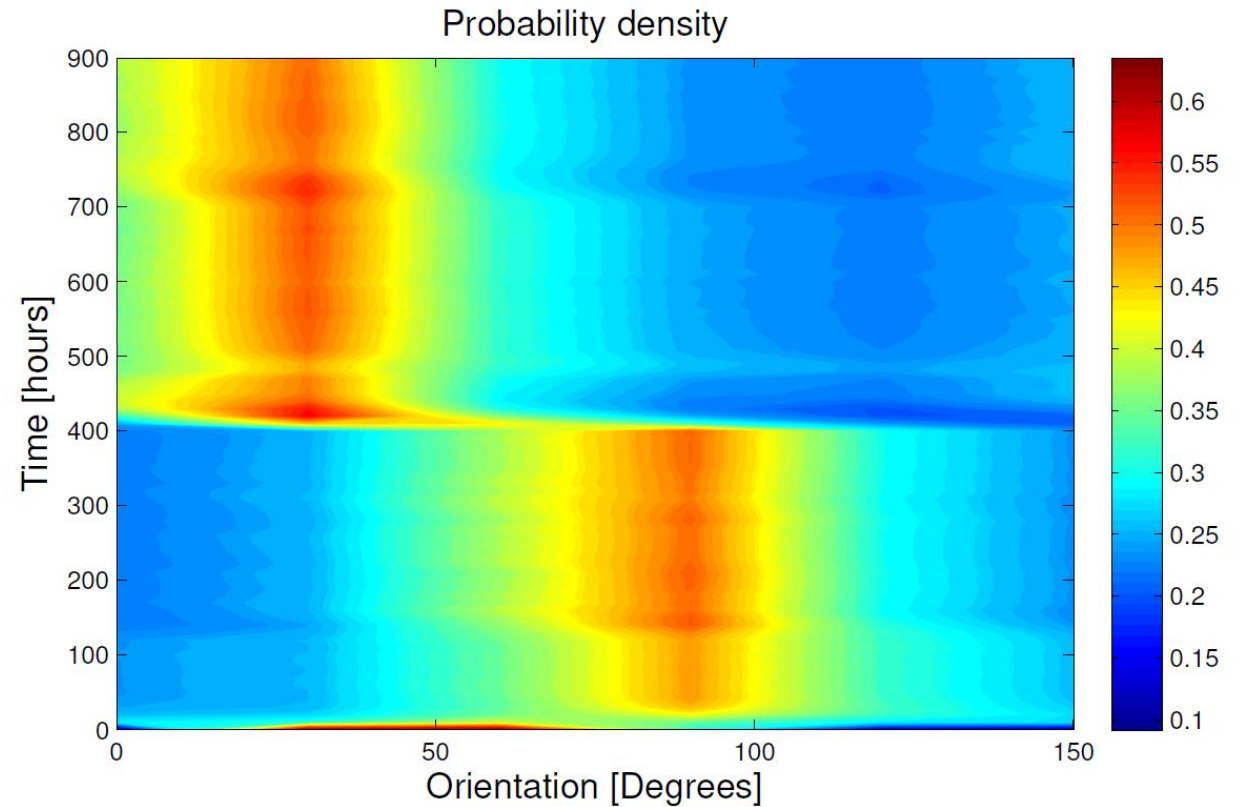
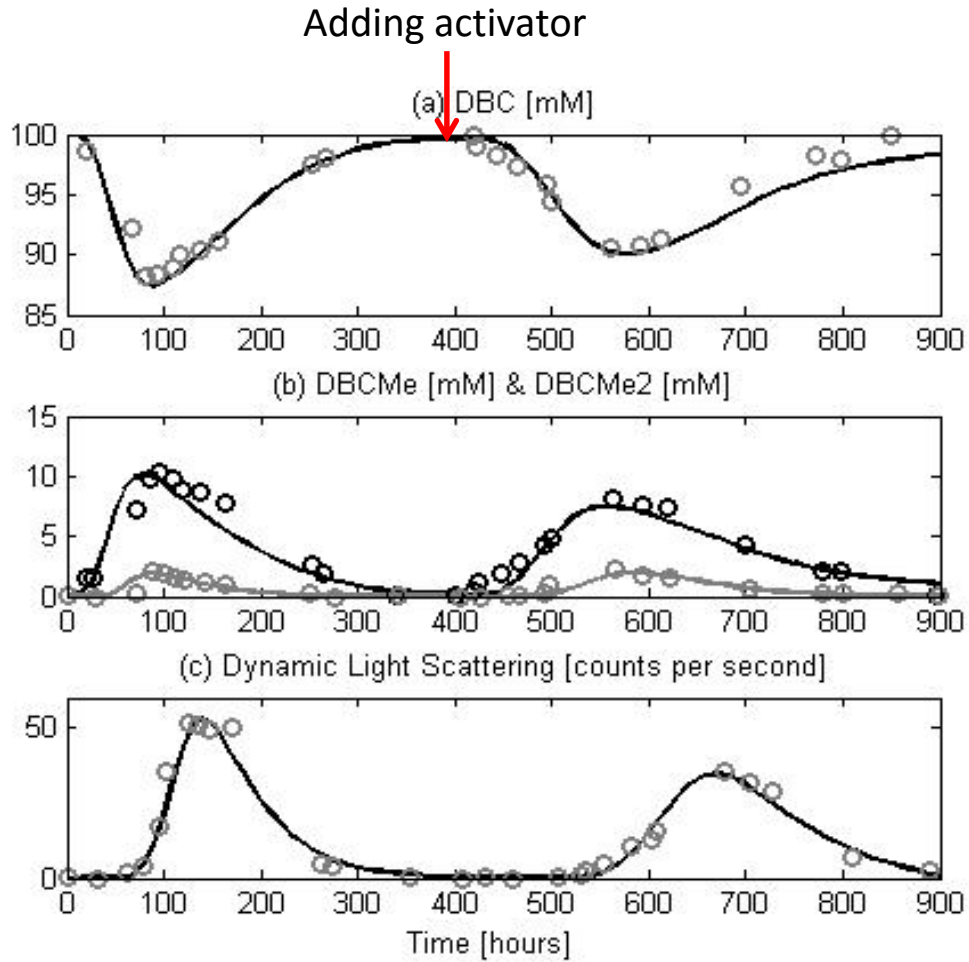
$$\frac{\partial p_n(\mathbf{\Gamma}_n, t)}{\partial t} = \sum_{i=1}^4 D_i \frac{\partial}{\partial \Gamma_n^{(i)}} \left[\frac{\partial p_n^{(i)}}{\partial \Gamma_n^{(i)}} + p_n^{(i)} \frac{\partial \ln \psi_n^{(i)}}{\partial \Gamma_n^{(i)}} + \frac{p_n^{(i)}}{k_B T} \frac{\partial \phi_n^{(i)}}{\partial \Gamma_n^{(i)}} \right]$$

Second-order structures:

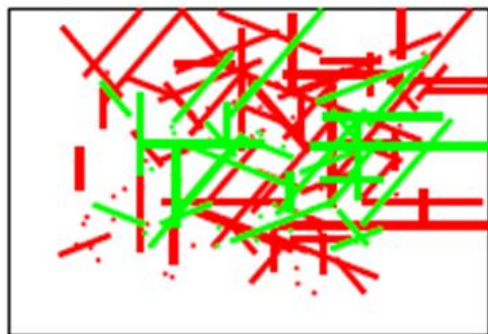
$$\frac{\partial q_n(\mathbf{\Gamma}'_n, t)}{\partial t} = \sum_{i=1}^2 D_{s,i} \frac{\partial}{\partial \Gamma_n'^{(i)}} \cdot \left[\frac{\partial q_n^{(i)}}{\partial \Gamma_n'^{(i)}} + q_n^{(i)} \frac{\partial \ln \psi_n'^{(i)}}{\partial \Gamma_n'^{(i)}} + \frac{q_n^{(i)}}{k_B T} \frac{\partial \phi_n'^{(i)}}{\partial \Gamma_n'^{(i)}} \right]$$

RESULTS

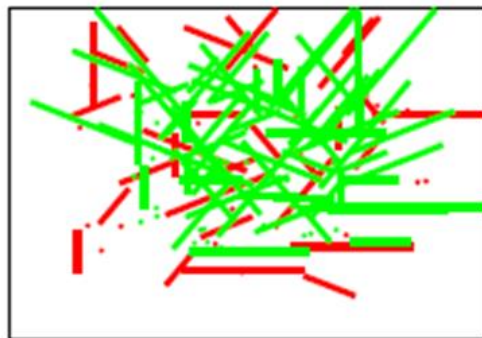
Coarse-graining in the reaction coordinates



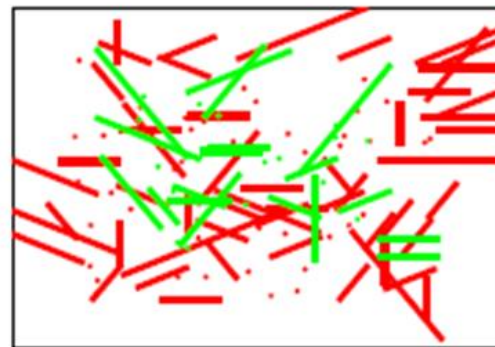
(a) 100 hours



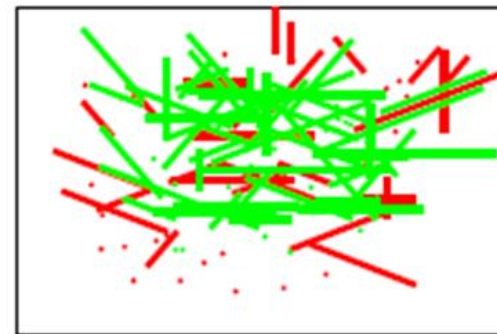
(b) 200 hours



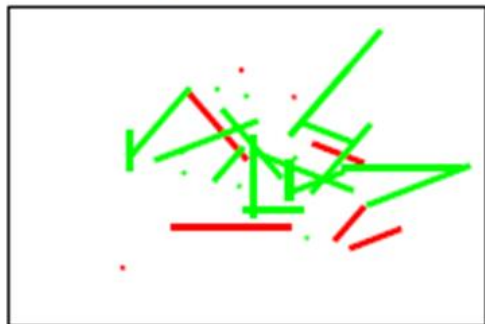
(e) 600 hours



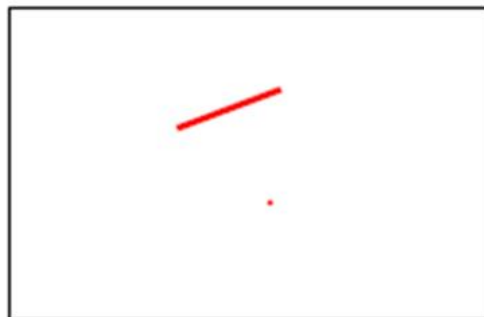
(f) 700 hours



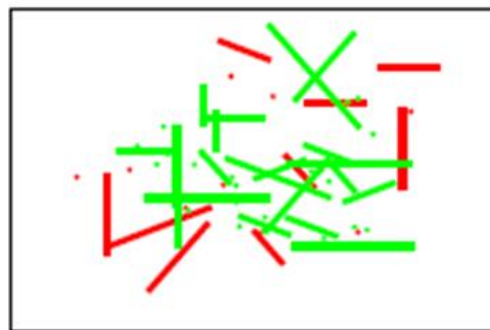
(c) 300 hours



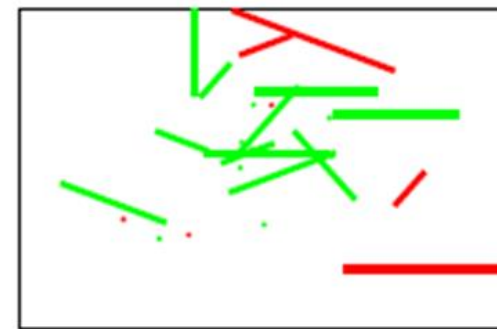
(d) 500 hours



(g) 800 hours



(h) 900 hours



Entropy production rate

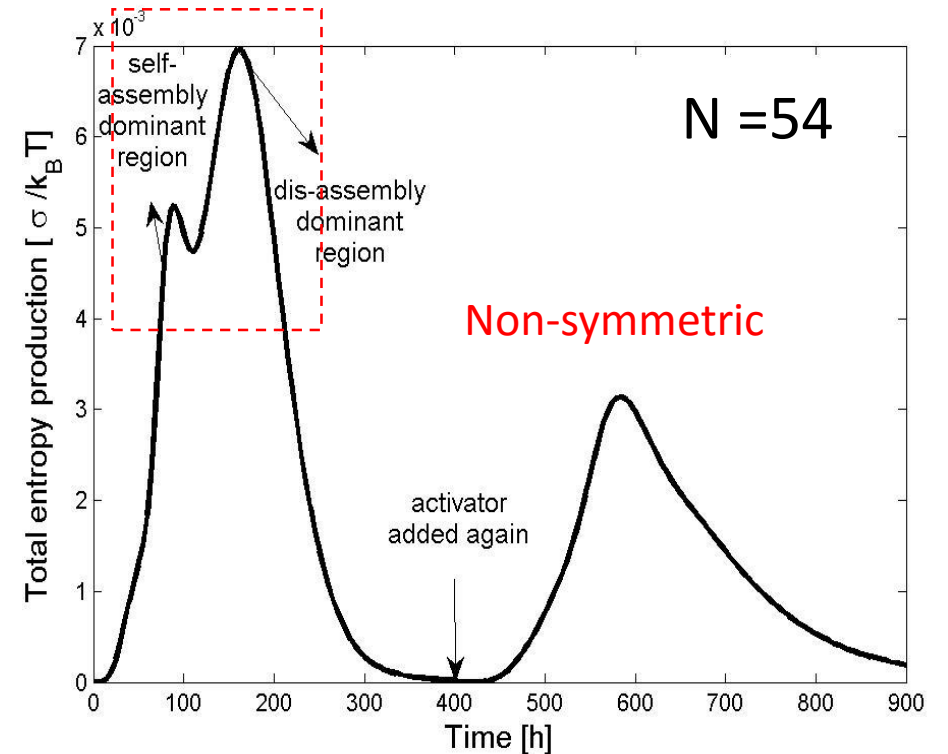
$$\sigma(t; \eta) = -\frac{1}{T} \int_{\Gamma} \vec{J}_{\Gamma}(\Gamma, t; \eta) \cdot \nabla_{\Gamma} \mu(\Gamma, t; \eta) d\Gamma$$

↓

$$\sigma(t; \eta) = \sum_j k_j (\Delta_j \mathcal{Z}(t; \eta))^2$$

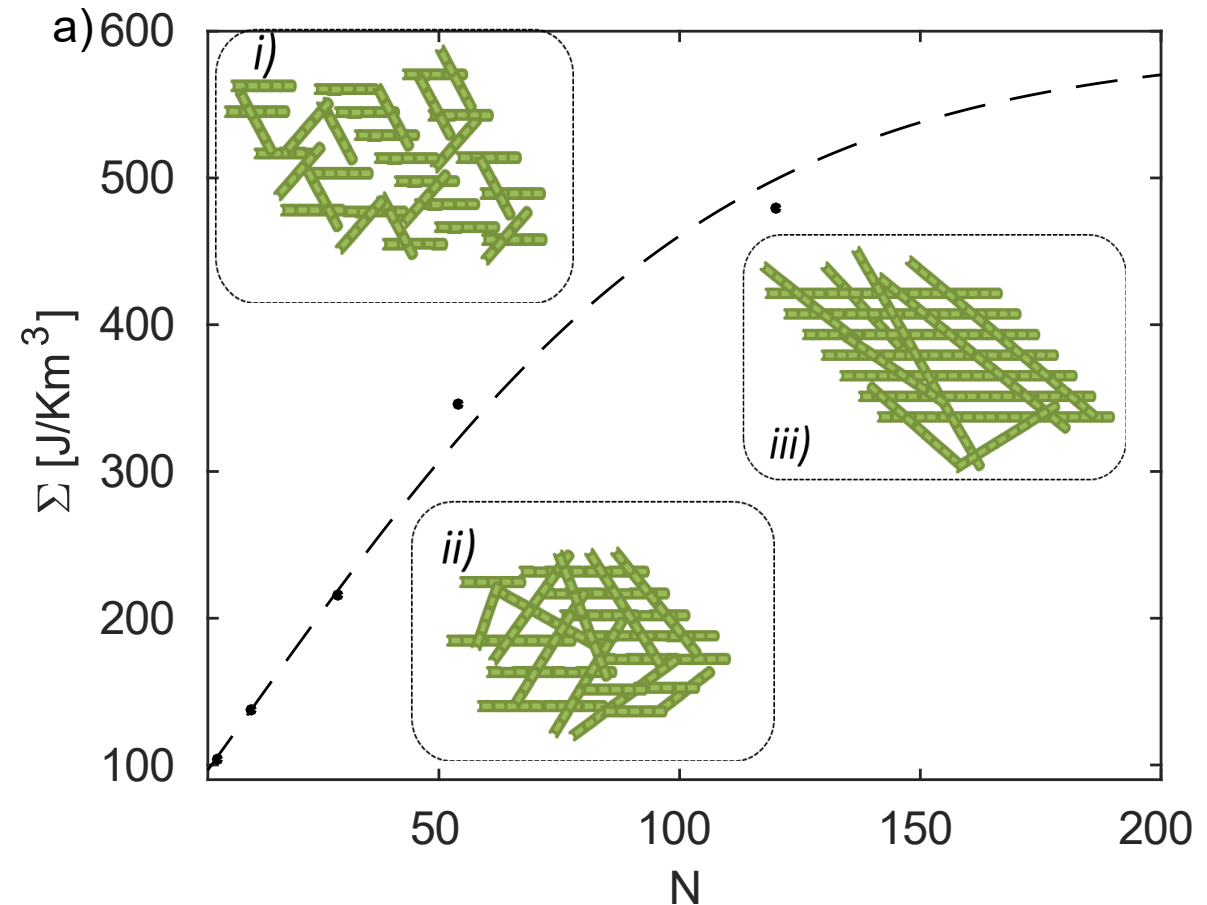
↓

$$\sigma_g(t; N) = \sum_{i=1}^2 \sigma_{0,i} + \sum_{n=2}^N \sum_{i=1}^4 \sigma_{1,i}^{(n)} + \sum_{n=2}^{\infty} \left[\sum_{m=2}^{\infty} \sigma_{2,1}^{(n,m)} + \sum_{y=1}^{n-1} \sigma_{2,2}^{(n,n-y)} \right]$$



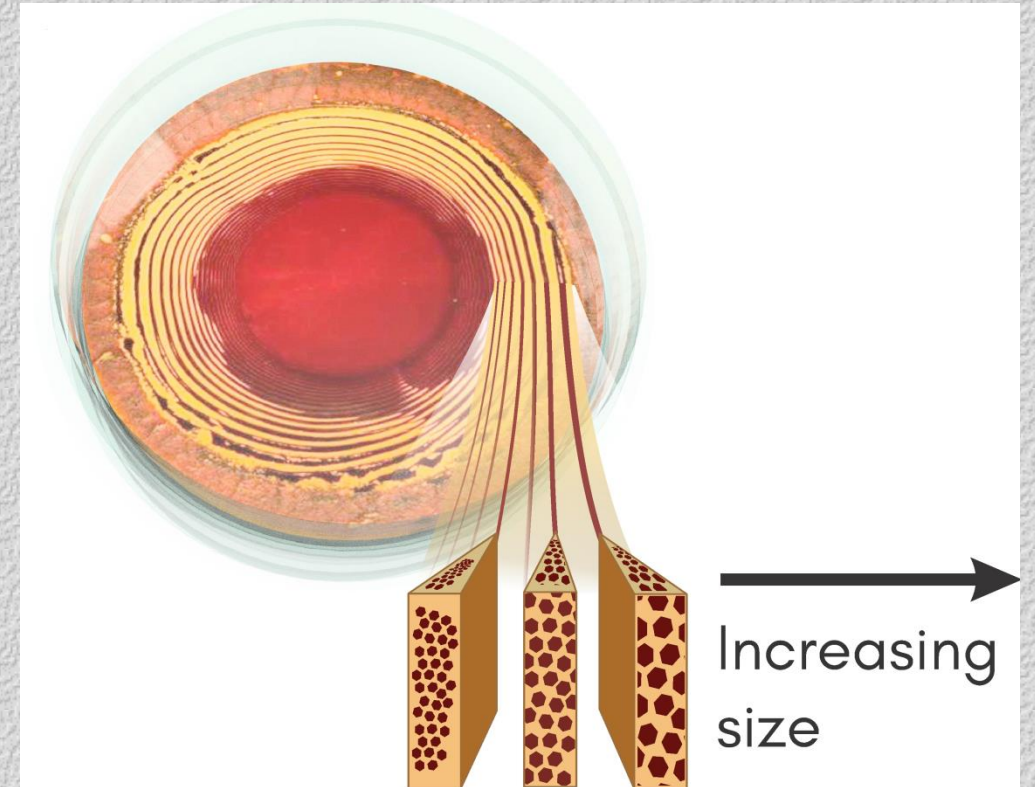
$$\Sigma(\eta) = \int_0^\tau \int_{\vec{r}} \sigma(\vec{r}, t; \eta) d\vec{r} dt$$

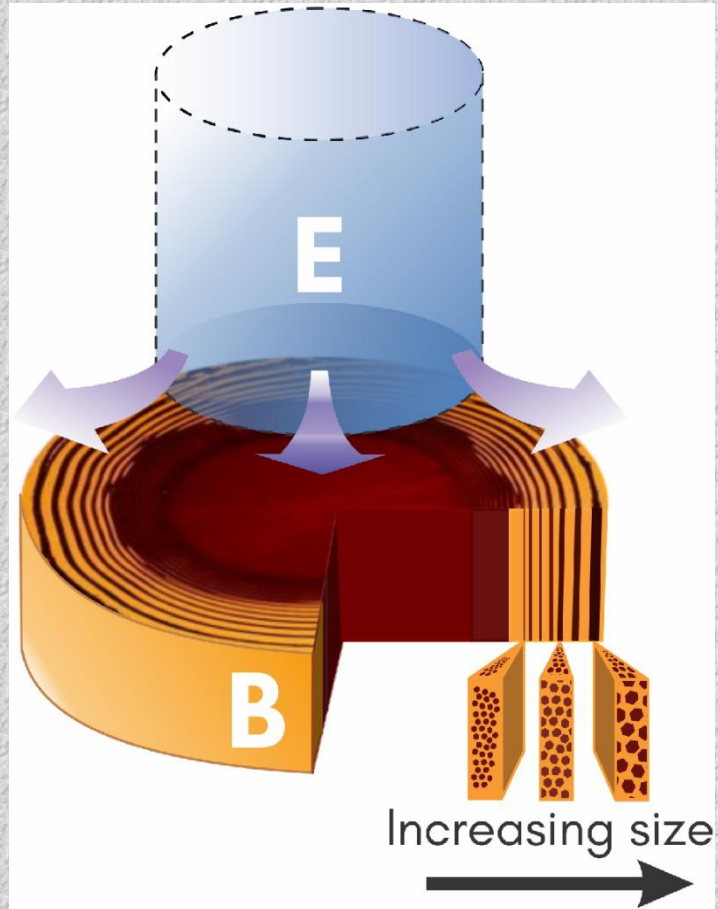
The total entropy produced increases monotonically but **not linearly**. From experimental results, we observe that **this quantity is maximized**.



Liesegang rings

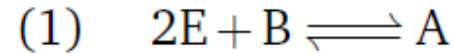
- ❖ Periodic precipitation pattern.
- ❖ Their **control** and **engineering** constitute a crucial task for applications.
- ❖ Liesegang patterns are composed of **mono-disperse nano- and micro-structures** whose size varies predictably from ring to ring.



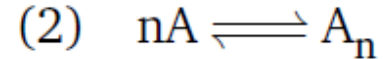


- ❖ Electrolyte E **diffuses** into the matrix and interacts with electrolyte B to trigger the **bottom-up self-assembly** of meso-structures leading to the Liesegang patterns.
- ❖ **Structures size** increases as a function of the radial position.

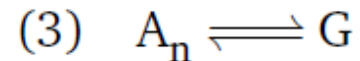
Mechanism



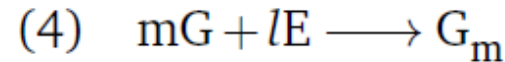
(1) First order activation (chemical reaction)



(2) First order self-assembly (chemical reaction/pre-nucleation)



(3) Second order activation (phase change)



(4) Second order self-assembly (aggregation)

$$R_1 = k_1^+(T)C_B C_E^2 - k_1^-(T)C_A,$$

E: activator (silver nitrate)

B: disactivated BB (potassium dichromate)

A: activated BB (silver dichromate)

A_n: first order structure

G_m: second order structure

$$R_2 = k_2^+(T)C_A^2 - k_2^-(T)C_{A_n},$$

$$R_3 = k_3^+(T)C_{A_n}^2 - k_3^-(T)C_G$$

$$R_4 = \begin{cases} k_4(T)C_G C_{G_m}^2 & \text{if } C_G < C_{lim} \\ k_4(T)C_G C_{G_m}^2 + k_4(T)C_E C_G (C_G - C_{lim}) & \text{if } C_G \geq C_{lim} \end{cases}$$

Model

A. Arango, JMR, D. Barragan, PCCP, 20, 4699 (2018)

Continuity equation

$$\frac{\partial p_i(\mathbf{\Gamma}, t)}{\partial t} = -\nabla_{\mathbf{\Gamma}} \cdot \mathbf{J}_i(\mathbf{\Gamma}, t),$$



$$\frac{\partial C_i(r, t)}{\partial t} = -\frac{1}{r} \frac{\partial}{\partial r} r J_i^{(d)}(r, t) - \sum_{j=1}^4 \dot{r}_{i,j}(r, t),$$

Experiments:

$$\frac{\Delta d}{\Delta C_E} \propto -1/C_E$$

Energy Balance

$$\frac{\partial e(r, t)}{\partial t} = -\frac{1}{r} \frac{\partial}{\partial r} r J_e(r, t),$$

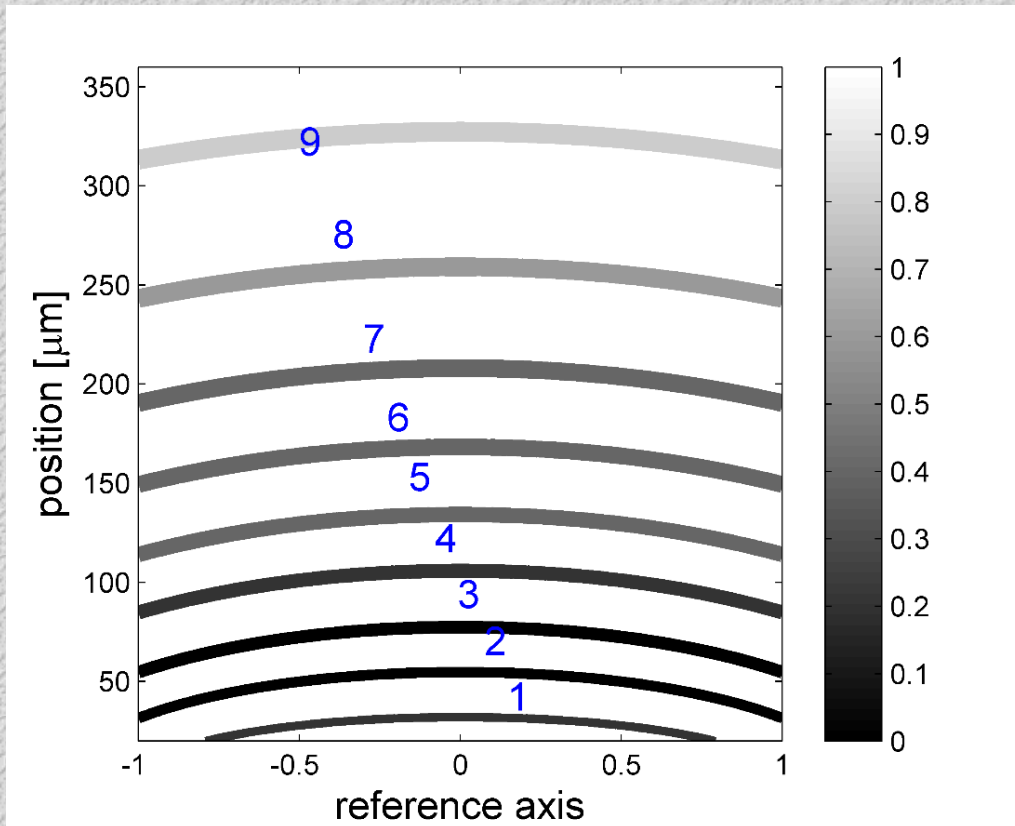


$$\sum_i C_i c_{P,i} \frac{\partial T(r, t)}{\partial t} = -\frac{1}{r} \frac{\partial}{\partial r} r J_e(r, t) + \sum_i h_i \frac{1}{r} \frac{\partial}{\partial r} r J_{d,i}(r, t) - \sum_{j=1}^4 \Delta h_j R_j,$$

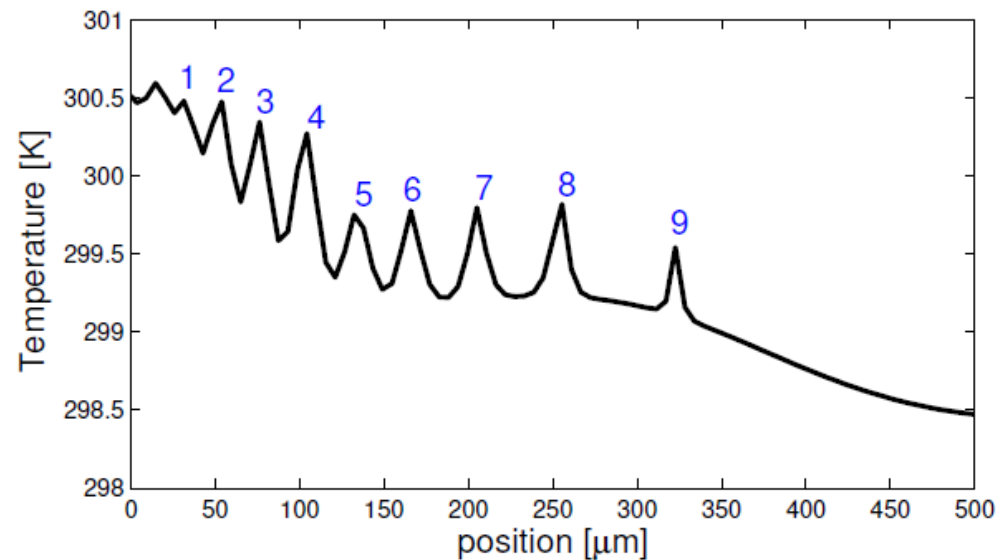
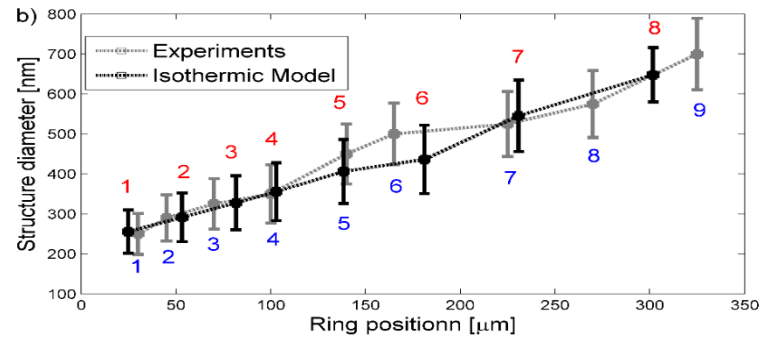
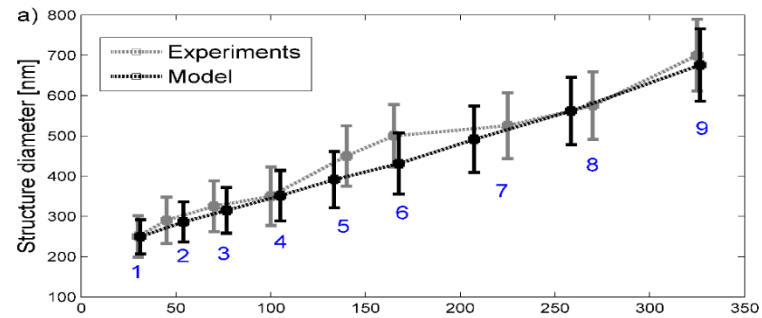
Structure size:

$$d(r, t) = d_0 + \omega \ln(C_E(r_{lim}, 0)/C_E(r, t)), \quad \forall r > r_{lim},$$

Results



- ❖ Ring distribution obtained from our model at time t_p (smaller than relaxation time).
- ❖ Darker color corresponds to the highest concentration of precipitated structures while the lighter color indicates absence of structure.
- ❖ From the experiments, we estimate ω and d_0 .

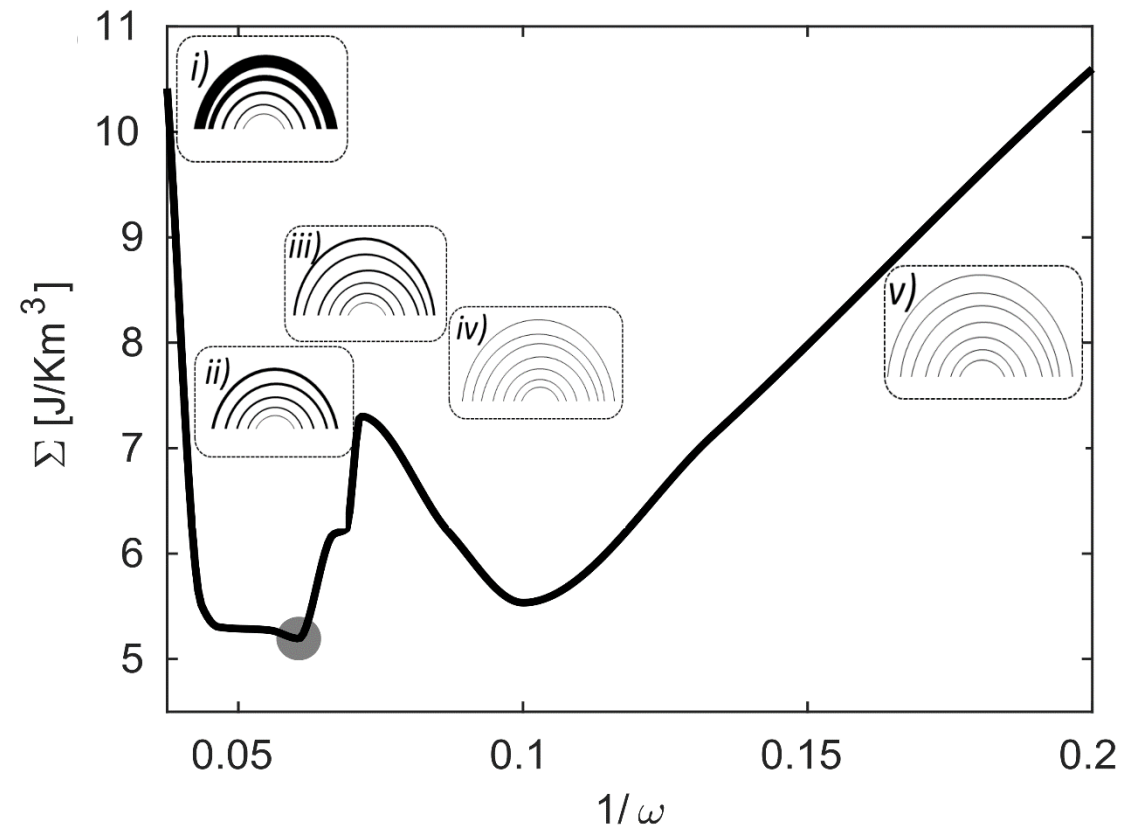


- ❖ We observe a ring distribution in which the **separation** between the rings **increases** with the distance.
- ❖ The **diameter** of the structure and its **standard deviation** as a function of position tends to **increase**.
- ❖ The error in the estimated position and in the structure's diameter is lower in the non-isothermal model.

Entropy produced

$$\sigma_L(r,t;\omega) = \frac{\kappa}{T^2} \left(\frac{\partial T}{\partial r} \right)^2 + \sum_k \frac{\mathcal{D}_k}{T} \left(\frac{\partial C_k}{\partial r} \right)^2 + \frac{1}{T} \sum_{i=1}^4 J_i^2(\omega)/k^+$$

- ❖ The system evolves towards a structure which **minimizes the lost work** in its formation.
- ❖ The structure thus adopts an **architecture** such that the work lost in **changing the configuration** is almost negligible



CONCLUSIONS

- ❖ Models based on **mesoscopic thermodynamics** enable us to understand and to **describe the evolution** of the **internal architecture** of meso-structures.
- ❖ The model allow us to **compute the entropy production** of the NESA process as a function of the **structural parameter**.
- ❖ The structures observed in this system are found at **extreme values of the entropy produced** when represented as a function of a **structural parameter**.

BOUNDARY CONDITIONS

First-order structures:

$$\begin{aligned} \left. \frac{\partial p_n}{\partial \Gamma_n^{(\gamma)}} \right|_{\Gamma_n=0} &= \left. \frac{\partial p_n}{\partial \Gamma_n^{(\gamma')}} \right|_{\Gamma_n=0} = \left. \frac{\partial p_n}{\partial \Gamma_n^{(\lambda)}} \right|_{\Gamma_n=0} = \left. \frac{\partial p_n}{\partial \Gamma_n^{(\theta)}} \right|_{\Gamma_n=0} \\ &= J_{n-1}^{(\gamma)}(1, t) + J_{n+1}^{(\gamma')}(1, t) + J_n^{(\theta)}(\pi, t) \end{aligned}$$

Second-order structures:

$$\begin{aligned} \left. \frac{\partial q_n}{\partial \Gamma_n^{(\gamma_1)}} \right|_{\Gamma'_n=0} &= \dots = \left. \frac{\partial q_n}{\partial \Gamma_n^{(\gamma_m)}} \right|_{\Gamma'_n=0} = \dots = \left. \frac{\partial q_n}{\partial \Gamma_n^{(\gamma_{\lfloor n/2 \rfloor})}} \right|_{\Gamma'_n=0} = \\ \left. \frac{\partial q_n}{\partial \Gamma_n^{(\gamma'_N)}} \right|_{\Gamma'_n=0} &= \dots = \left. \frac{\partial q_n}{\partial \Gamma_n^{(\gamma'_y)}} \right|_{\Gamma'_n=0} = \dots = \left. \frac{\partial q_n}{\partial \Gamma_n^{(\gamma'_{n+1})}} \right|_{\Gamma'_n=0} = \\ &J_n^{(\lambda)}(1, t) + \sum_{m=1}^{\lfloor n/2 \rfloor} J_m^{(\gamma_n)}(1, t) + \sum_{y=n+1}^N J_y^{(\gamma'_n)}(1, t) \end{aligned}$$

Modelling potential barriers

A \square B

A: $\gamma < \gamma^*$

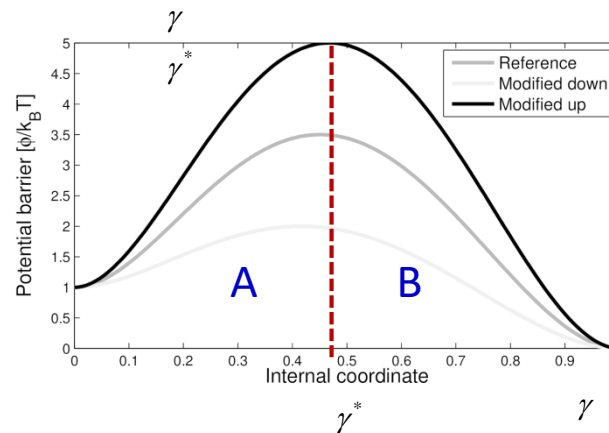
B: $\gamma \geq \gamma^*$

$$\begin{aligned}\phi(0) &= \mu_A^0 \\ \phi(1) &= \mu_B^0 \\ \phi(\gamma^*) &= \max(\phi(\gamma)) - \mu_A^0 = \epsilon \\ \left. \frac{d\phi(\gamma)}{d\gamma} \right|_{\gamma=0} &= 0 \\ \left. \frac{d\phi(\gamma)}{d\gamma} \right|_{\gamma=1} &= 0 \\ \left. \frac{d\phi(\gamma)}{d\gamma} \right|_{\gamma=\gamma^*} &= 0\end{aligned}$$

$$\exp((\mu_A^0 - \mu_B^0)/RT) = \frac{P_{B,eq}}{P_{A,eq}} = \frac{\int_{\gamma^*}^1 \exp(-\phi(\gamma)/RT) d\gamma}{\int_0^{\gamma^*} \exp(-\phi(\gamma)/RT) d\gamma}$$

$$\phi(\gamma) = \sum_{i=0}^5 c_i \gamma^i$$

Bistable



$$\int_0^{\gamma_m} \exp(\phi(\gamma)/RT) d\gamma \approx \exp(E_a/RT)$$

Modelling a potential barrier with an intermediate state

$$\phi(\gamma) = \begin{cases} \phi^-(\gamma) & 0 \leq \gamma \leq \gamma_{ES} \\ \phi^+(\gamma) & \gamma_{ES} \leq \gamma \leq 1 \end{cases}$$

$$\left. \frac{d\phi^-(\gamma)}{d\gamma} \right|_{\gamma=0} = 0$$

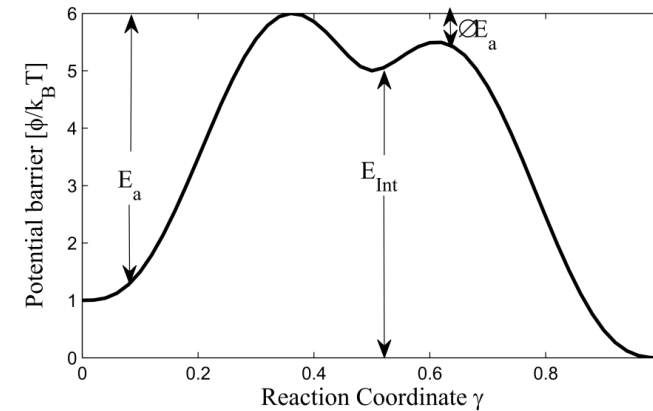
$$\left. \frac{d\phi^-(\gamma)}{d\gamma} \right|_{\gamma=\gamma_{ES}} = 0$$

$$\left. \frac{d\phi^-(\gamma)}{d\gamma} \right|_{\gamma=\gamma_-^*} = 0$$

$$\phi(0) = \mu_S^0$$

$$\phi(\gamma_{ES}) = \mu_{ES}^0$$

$$\phi(\gamma_-^*) = \max(\phi^-(\gamma)) - \mu_S^0 = \epsilon^-$$



$$\exp((\mu_S^0 - \mu_{ES}^0)/RT) = \frac{P_{ES,eq}}{P_{S,eq}} = \frac{\int_{\gamma_-^*}^{\gamma_{ES}} \exp(-\phi^-(\gamma)/RT) d\gamma + \int_{\gamma_{ES}}^{\gamma_+^*} \exp(-\phi^+(\gamma)/RT) d\gamma}{\int_0^{\gamma_-^*} \exp(-\phi^-(\gamma)/RT) d\gamma}$$

$$\phi(\gamma_{ES}) = \mu_{ES}^0$$

$$\phi(1) = \mu_P^0$$

$$\phi(\gamma_+^*) = \max(\phi^+(\gamma)) - \mu_S^0 = \epsilon^+$$

$$\left. \frac{d\phi^+(\gamma)}{d\gamma} \right|_{\gamma=1} = 0$$

$$\left. \frac{d\phi^+(\gamma)}{d\gamma} \right|_{\gamma=\gamma_{ES}} = 0$$

$$\left. \frac{d\phi^+(\gamma)}{d\gamma} \right|_{\gamma=\gamma_+^*} = 0$$

$$\exp((\mu_S^0 - \mu_P^0)/RT) = \frac{P_{P,eq}}{P_{S,eq}} = \frac{\int_{\gamma_{ES}}^{\gamma_+^*} \exp(-\phi^+(\gamma)/RT) d\gamma}{\int_0^{\gamma_-^*} \exp(-\phi^-(\gamma)/RT) d\gamma}$$